International Journal of Thermofluid Science and Technology (2024)
Volume 11, Issue 2, Paper No. 110204
https://doi.org/10.36963/IJTST.2024110204
Research Article

Impact of wall electrical conductivity on heat transfer enhancement in MHD hybrid nanofluid flow within an annulus

Ali Bendjaghlouli[1], Brahim Mahfoud [2*], Hibet Errahmane Mahfoud[3]

[1] *Faculty of Mechanical Engineering, Abdelhafid Boussouf University Center in Mila,43000, Algeria*
[2] *Mechanical Engineering Department, University of Bouira, 10000, Algeria.*
[3] *Department of Natural and Life Sciences, Univesity20 août 1955–Skikda, 21000, Algeria*

ARTICLE INFO

Received: 24 Mar. 2024;
Received in revised form:
30 May 2024;
Accepted: 01 June 2024;
Published online:
05 June 2024

Keywords:
Coaxial cylinders, heat transfer, hybrid nanofluid, magnetic field, swirling flow

ABSTRACT

A numerical investigation was conducted to explore the influence of magnetic field and the electric conductivity of container walls on the swirling flow of a hybrid nanofluid. In this study, a stationary inner wall and a rotating outer wall with a fixed Ω were considered within the annular between coaxial cylinders. Radial application of a magnetic field was utilized to assess its impact on the average Nusselt number. The mathematical model, formulated by differential equations, was solved using the finite volume method. The study examined the variations in azimuthal velocity, temperature, and Nusselt number with increasing magnetic intensity. Therefore, it can be concluded that the control of heat transfer efficiency increasingly relies on the combined influence of magnetic field intensity and the electrical conductivity of walls. The findings revealed that higher magnetic Hartmann numbers led to elevated temperature distribution and azimuthal velocity within the annulus center. Moreover, electromagnetic damping exhibited a more pronounced impact on heat transfer when all walls were electrically conductive, resulting in a 90% improvement in heat transfer with the hybrid nanofluid.

1. Introduction

The utilization of hybrid nanofluids in modern industry has emerged as a promising strategy for enhancing heat transfer efficiency in various applications. Hybrid nanofluids, consisting of a base fluid with dispersed nanoparticles, offer unique thermal properties, significantly improving heat transfer compared to conventional fluids. Several notable papers introducing simulations of heat and mass transfer of hybrid nanofluids in this field can be found in references [1–6]. These nanofluids enhance thermal conductivity, convective heat transfer coefficients, and heat capacity, making them ideal for heat exchange systems in diverse industrial processes like cooling systems and thermal energy storage. Incorporating hybrid nanofluids into industrial equipment can achieve higher heat transfer rates, and improved energy, contributing to modern industrial practices' advancement and sustainability [7–9].

[*]*Corresponding e-mail*: *b.mahfoud@univ-bouira.dz* (B.Mahfoud)

Nomenclature

B	magnitude of the external magnetic field (Tesla)	*Greek symbols*	
H	height of the cylinder (m)	α	Thermal diffusivity of the fluid (m^2/s)
Ha	Hartmann number	β	thermal expansion coefficient (1/K)
Nu	localNusselt number	Θ	Dimensionless temperature
$\overline{Nu}$	averageNusseltnumber	v	Kinematic viscosity of the fluid (m^2/s)
P	dimensionless pressure	λ	thermal conductivity (w/ m. C)
Pr	Prandtl number	ρ	density of the fluid (kg/m^3)
R	annular gap	σ	electric conductivity (Ω /m)
r, θ, z	dimensionless spatial coordinates	Φ	dimensionless electric potential
r_i	inner radius(m)	Ω	angular velocity (rad/s)
r_o	outer radius(m)	ϕ	volume fraction
Re	Reynolds number	*Subscripts*	
Ra	Rayleigh number	f	fluid
T	temperature (K)	p	solid phase
u,v,w	dimensionless radial, axial, azimuthal velocity components	nf	nanofluid
U	coefficient of determination	hnf	hybrid nanofluid

Ongoing research continues to explore potential applications and optimization of hybrid nanofluids to further enhance heat transfer performance across various industrial sectors [10-11].

Recently, research focus has shifted towards hybrid nanofluids due to their potential for enhancing heat transfer rates. Despite this, research on hybrid nanofluids remains relatively limited, with ongoing experimental studies exploring their properties and applications. Recent advancements in hybrid nanofluid research reflect a heightened interest in this field, with ongoing experimental studies indicating an intensified exploration [12].

Fluid circulation in annular geometries offers numerous benefits across various industrial applications, including cooling in electronics. Annular geometries provide an effective solution for efficient heat dissipation, essential for maintaining optimal performance and prolonging component lifespan in electronics. Circulating fluid through an annular space enhances heat transfer through increased surface area contact between the fluid and heated components, resulting in more efficient cooling and temperature regulation [13-16]. Annular geometries also allow for compact designs and efficient space utilization, making them suitable for applications with significant size and weight constraints [17-21].

Research into the behavior of fluids under magnetic field influence, known as magnetohydrodynamics (MHD), has gained significant attention due to its broad applications in medical and industrial contexts. The interaction between magnetic fields and electrically conductive fluids generates a resistive force called the Lorentz force, crucial for applications like nuclear reactor cooling. Both liquid metals and nanofluids enhance heat transfer and cooling processes, offering potential advancements in cooling technologies [22-26]. Researchers are interested in studying nanofluids in rotating environments under a magnetic field, employing numerical and analytical approaches to explore their intricate relationship. In recent studies, researchers have conducted experiments involving the addition of two or more types of nano-sized particles

into the same base liquid, resulting in what is known as a hybrid nanofluid [27-28]. This combination of nanoparticles in a single base liquid introduces unique properties not found in individual nanomaterials. References [29–33] include recent research on magnetohydrodynamic (MHD) flow of nanofluids, as well as studies on MHD flow over a stretching surface and a stretching porous sheet. These studies provide valuable insights into the complex MHD mixed convection flow behavior of nanofluid on a permeable stretching sheet, with implications for various industrial applications. In references [34-36], discussions revolve around heat transfer enhancement in boundary layer flow of hybrid nanofluids attributed to variable viscosity and natural convection, as well as magnetohydrodynamic (MHD) nanofluid flow influenced by gyrotactic microorganisms. Madani et al. [37] focused on studying heat transfer via natural convection of nanofluids in an electrically conductive enclosure. This study aims to demonstrate the importance of wall electrical conductivity in enhancing heat transfer in swirling nanofluid flow within an enclosure. Additionally, the study seeks to determine the maximum magnetic field intensity associated with enhanced heat transfer and identify the optimal scenario among the four cases studied.

The motivation behind the present work lies in the fact that there is limited research focusing on cooling hybrid nanofluids in annular geometries with swirl flow under the influence of a magnetic field. The novelty contribution is exploring the behavior of hybrid nanofluids under radial magnetic fields through numerical simulations. Additionally, these studies aim to analyze the impact of parameters such as magnetic field strength and electrical conductivity on temperature distribution, velocity, and Nusselt number.

2. Definition and mathematical model

The present study delves into the analysis of mixed convection flow within an annulus formed between two coaxial cylinders. The hybrid fluid consists of copper (Cu) and graphene oxide (GO) nanoparticles dispersed within a kerosene oil base fluid moving in this annulus. While the outer cylinder rotates at an angular velocity Ω, the inner cylinder remains static. The annular geometry is characterized by R = 1 - (ri/ro), where ri and ro represent the radii of the inner and outer cylinders, respectively.

Numerical simulations are executed under specified conditions, featuring an aspect ratio $A=H/r_o$ of 1 and an annular gap R=0.9. These simulations entail the consistent imposition of a radial magnetic field denoted as B0. Additionally, the outer cylinder maintains a heat temperature Th slightly higher than that of the inner wall temperature (T_c), as illustrated in Fig . 1. The study compares two scenarios: one where electrical insulation is assumed, and the other where all walls are considered electrically conducting. Furthermore, the physical model is scrutinized based on several assumptions, including laminar flow and neglecting joule heating, thermal radiation, viscosity dissipation, and the Hall effect. The nanoparticles, characterized by cylindrical shape (with n=6), exhibit uniform size distribution within the nanoparticle dispersion (Table 2)**.** Both the base fluid and nanoparticles are managed to maintain thermal equilibrium. The hybrid nanofluid consists of GO-Cu nanoparticles suspended in a kerosene oil (50% - 50%) mixture (Table 1).

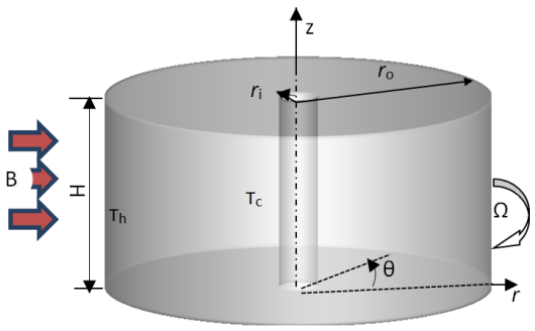

Fig. 1 Geometry of model

Table .1 Thermo-physical properties [9]

Parameter	hybrid nanofluid
Density	$\rho_{hnf} = (1-\varphi_2)\left[(1-\varphi_1)\rho_f + \varphi_1\rho_{P1}\right] + \varphi_2\rho_{P2}$
Dynamic viscosity	$\mu_{hnf} = \frac{\mu_f}{(1-\varphi_1)^{2.5}(1-\varphi_2)^{2.5}}$
Heat capacity	$(\rho C_p)_{hnf} = (1-\varphi_2)\left[(1-\varphi_1)(\rho C_p)_f + \varphi_1(\rho C_p)_{P1}\right] + \varphi_2(\rho C_p)_{P2}$
Expansion coefficient	$(\rho\beta)_{hnf} = (1-\varphi_2)\left[(1-\varphi_1)(\rho\beta)_f + \varphi_1(\rho\beta)_{P1}\right] + \varphi_2(\rho\beta)_{P2}$
Conductivity	$\frac{k_{hnf}}{k_{nf}} = \left[\frac{k_{P2}+(n-1)k_{nf}-(n-1)(k_{nf}-k_{p2})\varphi_2}{k_{p2}+(n-1)k_{nf}+\varphi_2(k_{nf}-k_{p2})}\right]$, Where $\frac{k_{nf}}{k_f} = \left[\frac{k_{P1}+(n-1)k_f-(n-1)(k_f-k_{p1})\varphi_1}{k_{p1}+(n-1)k_f+\varphi_1(k_f-k_{p1})}\right]$
Electrical conductivity	$\sigma_{hnf} = \sigma_{nf}\left[\frac{\sigma_{p2}+2\sigma_{nf}-2\varphi_2(\sigma_{nf}-\sigma_{p2})}{\sigma_{p2}+2\sigma_{nf}+\varphi_2(\sigma_{nf}-\sigma_{p2})}\right]$, Where $\sigma_{nf} = \sigma_f\left[\frac{\sigma_{p1}+2\sigma_f-2\varphi_1(\sigma_f-\sigma_{p1})}{\sigma_{p1}+2\sigma_f+\varphi_1(\sigma_f-\sigma_{p1})}\right]$

Table 2 Properties of the base fluid and nanoparticles (Cu, GO)

Substances	(Kerosene-oil)[26]	(Cu)[14]	(GO)[28]
μ(kg/m.s)	0.00164	-	-
Cp(J/kg.K)	2090	385	717
κ(W/m.K)	0.145	401	5000
σ(S/m)	50	5.96×10^{7}	6.3×10^{7}
ρ(kg/m^3	783	8933	1880
β(1/K)	9.6×10^{-4}	1.67×10^{-5}	2.84×10^{-4}

Scaling is applied to length, velocity, pressure, and electric potential by r_o , Ωr_o , $\rho_f(\Omega r_o)^2$, and $B_0\Omega {r_o}^2$, respectively.. Consequently, the governing equations for the hybrid nanofluid are expressed in steady flow conditions.

- Mass conservation

$$\nabla U = 0 \quad (1)$$

- Momentum conservation law:

$$U.\nabla U + \nabla P = +\frac{1}{Re_f}\left(\frac{\mu_{hnf}\rho_f}{\mu_f\rho_{hnf}}\right)\nabla^2 U + \left(\frac{Ra_f}{Pr_f Re_f^2}\right)\left(\frac{(\rho\beta)_{hnf}}{\beta_f\rho_{hnf}}\right)\Theta + \left(\frac{\sigma_{hnf}\rho_f}{\sigma_f\rho_{hnf}}\right)\frac{{Ha_f}^2}{Re_f}(\vec{J}\times\vec{B}) \quad (2)$$

- Energy conservation:

$$U.\nabla\Theta = \frac{\alpha_{hnf}}{\alpha_f Re_f Pr_f}(\nabla^2\Theta) \quad (3)$$

The presence of a magnetic field interacting with a convective flow can lead to the generation of an electric current, a concept elucidated by Faraday's law of electromagnetic induction. This occurrence arises from the relative movement between a conductor (or conducting fluid) and the magnetic field, generating an electromotive force (EMF) and consequently inducing an electric current (J). In elucidating the electric potential's behavior (Φ), we can apply Ohm's law in the following express :

$$\nabla^2\Phi - \nabla.(U\times\vec{e}_r) = 0 \quad (4)$$

$$J = U\times\vec{e}_r - \nabla\Phi \quad (5)$$

$$F_M = \vec{J}\times\vec{B} \quad (6)$$

These parameters are defined as:

$$\begin{cases} Re_f = \frac{\Omega r_o^2}{\nu_f}, & \text{Reynolds number} \\ Ra_f = \frac{\beta_f g\Delta T r_o^3}{\nu_f\alpha_f}, & \text{Rayleigh number} \\ Ha_f = Br_o\sqrt{\frac{\sigma_f}{\rho_f\nu_f}}, & \text{Hartmann number} \\ Pr_f = \nu_f/\alpha_f, & \text{Prandtl number} \end{cases} \quad (7)$$

Considering the initial and boundary conditions, velocities along all walls are set to zero in compliance with the No-slip conditions. Adiabatic conditions are imposed on the upper and lower walls, while the exterior (T_h) and

interior (T_c) boundaries of the annulus maintain constant temperatures. In cases where all walls exhibit electrical conductivity, the boundary conditions for electric potential are intricately linked to the electrical properties of the wall, including its thickness and conductivity (ew, σw). The formulation for the electric potential is provided in reference [1].

$$J_r = -k_w \frac{\partial}{\partial r}(J_r) \quad (8)$$

$$-\frac{\partial \Phi}{\partial r} = -k_w \frac{\partial}{\partial r}\left(\frac{\partial \Phi}{\partial r}\right) \quad (9)$$

The magnetic boundary condition in the (EC-walls) case, after integration, can be expressed as :

$$\Phi = k_w \frac{\partial \Phi}{\partial r} \quad (10)$$

Here, the conductance ratio is denoted by :

$$k_w = \frac{\sigma_w e_w}{\sigma_{hnf}} R \, . \quad (11)$$

For the case of electrically insulated walls, the normal derivative of electric potential is set to zero, ensuring no electric current perpendicular to the interface between the fluid and insulating walls. This implies that the potential of the upper and lower disks is determined by the condition ($\partial\Phi/\partial z=0$).

The heat transfer is characterized by the local and average Nusselt numbers, denoted as:

$$\begin{cases} Nu(r,\theta) = \frac{k_{hnf}}{k_f}\left(\frac{\partial \Theta}{\partial z}\right)\Big|_{r=ri} \\ \overline{Nu} = \left(\frac{1}{\pi}\right)\int_0^1 \int_0^{2\pi} Nu\,(r,\theta) r d\theta dr \end{cases} \quad (10)$$

The boundary conditions are as:

- At the upper disk, $z = \frac{H}{r_o}$,

$U(u,v,w) = 0, \frac{\partial \Theta}{\partial z} = 0\,, \frac{\partial \Phi}{\partial z} = 0,$

- At the bottom disk $(z = 0)$

$U(u,v,w) = 0, \frac{\partial \Theta}{\partial z} = 0\,, \frac{\partial \Phi}{\partial z} = 0.$

- At the stationary inner wall $(r = r_i/r_o)$

-When all walls are electrically insulating

$U(u,v,w) = 0, \Theta = 0, \frac{\partial \Phi}{\partial z} = 0$ (EI-walls)

-When all walls are electrically conducting

$\Phi = k\frac{\partial \Phi}{\partial z}$ (EC-walls)

- At the rotating outer wall $(r = 1)$

$u = v = 0, w = 1\,, \Theta = 1\,,$

$\frac{\partial \Phi}{\partial z} = 0$ where (EI-walls)),

or $\Phi = k\frac{\partial \Phi}{\partial z}$, where (EC-walls).

- For geometrical symmetry are:

$U(r;\theta;\ z) = U(r;\ \theta + 2\pi;\ z).$

3. Calculation method and grid dimensions

The governing equations are discretized using the finite volume method, allowing for numerical solutions on a discrete grid. Specifically, the central difference method approximates diffusion terms, while the convective terms are handled using the QUICK technique [38]. The coupling between pressure and velocity is addressed using the SIMPLER algorithm. To evaluate grid dependence, simulations are conducted on three different meshes. As the Hartmann number (Ha) increases, the Hartmann layers near walls thin out, with a thickness of approximately ~1/Ha. Consequently, non-uniform grids are used for simulations with Ha values ranging from 0 to 50. Specifically, a grid of 55×100×55 nodes is employed for Ha values from 0 to 10, and 75×110×75 nodes for Ha exceeding 10. Grid independence is assessed by testing Ha values of 0 to 10, and Ha>10. Details of the grid and results for each case are summarized in Table 3. A comparison of average Nusselt values on the inner wall indicates changes smaller than 2%, confirming the appropriateness of the chosen grid. Convergence at each time step is considered achieved when the greatest residual error of the continuity equation across all control volumes falls below 10^{-5}.

Table3. Grid sizes test

0≤Ha≤10		*Ha>10*	
Mesh(r, θ, z)	$\overline{Nu}$	(*r, θ, z*)	$\overline{Nu}$
50×100×50	2.892	65×110×65	5.193
55×100×55	**2.734**	**75×110×75**	**5.012**
60×100×60	2.731	80×110×80	5.011

4. Results and discussion

The interplay of electrically conductive fluids with external magnetic fields sets fluid in motion via the Lorenz force. The presence of insulating walls greatly influences system behavior, giving rise to characteristic layers such as the Hartmann layer, which impedes fluid motion near conductive boundaries, and the Robert layer, promoting fluid mobility near insulating surfaces. Electromagnetic

stabilization is fundamental in comprehending how conducting fluids behave in magnetic fields, chiefly driven by induced electric currents due to the Lorentz force, notably observable in rotating fluid configurations like small and moderate cylinders.

In all simulations, the fluid is confined within a cylinder with a height-to-radius (H/R) ratio. Kerosene oil serves as the base fluid, with nanoparticles chosen to achieve a solid volume fraction (ϕ=0.01). The Reynolds number is maintained at Re = 1000, and calculations are conducted across various Hartmann numbers (0≤Ha≤50) and Raleigh numbers (Ra=10^5).

The primary aim of this section is to investigate the impact of magnetic fields on fluid characteristics, including Nusselt number (*Nu*), temperature (Θ), and azimuthal velocity (*w*). A comparison is drawn between the magnetic damping effects observed in a hybrid nanofluid and a kerosene oil-based fluid. Additionally, the section aims to elucidate the distinctions between scenarios with electrical insulation of all walls (EI walls) and perfect electrical conduction of all walls (EC walls)

4.1Validation

A comparison was conducted with the Alsaedi et al. [28] present numerical findings, depicted in Fig. 2, exploring the influence of magnetic parameters (M) on dimensionless temperature (Θ) within a numerical investigation on the flow of a hybrid nanofluid containing graphene oxide (GO) and copper (Cu) nanoparticles suspended in a Kerosene oil base fluid confined between two coaxial cylinders. The analysis demonstrates a decrease in temperature with higher magnetic field strengths. Furthermore, the comparison highlights a strong consistency among the derived values, with the maximum disparity falling below 2%, considered insignificant within the scope of a numerical analysis.

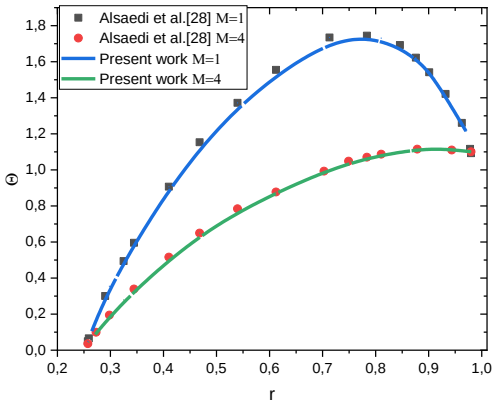

Fig. 2. Comparison with the numerical result of Alsaedi et al. [28], which gives Θ via M

4.2 Electrically insulating walls

In scenarios where all walls are insulating, electric current lines within the fluid form closed loops, contained by the insulating medium. The Hartmann layers predominantly concentrate on the inner and outer walls in this configuration. The presence of a radial magnetic field induces alterations in the convection of the nanofluid. This effect is attributed to the Hartmann layers near both the inner and outer walls, along with the development of Roberts layers near the bottom and top walls of the pool. The interplay of these layers and the radial magnetic field contributes to the observed changes in convection within the nanofluids.

Fig.3 elucidates the effects of an increasing magnetic field on the temperature (Θ) of Kerosene oil and hybrid nanofluid (GO /Cu/Kerosene oil) under the conditions of Ra=10^5 and Re=1000. Isothermal contours are depicted at the meridional plane (r=0) and the middle plane (z=1/2). The plot incorporates two values: Ha=0, represented by a solid line, and Ha=20, represented by a dashed line, superimposed on temperature (Θ) graphs.

The temperature contours exhibit a symmetrical shape at each Ha; however, they manifest different behaviors as Ha increases. For the case of Ha=0, where convection dominates the flow regime, buoyant forces generated due to fluid temperature differences cause the fluid to ascend in the middle and descend on the sides of the pool. For Ha=0, the

temperature distribution becomes round and exhibits two peaks, the first one adjacent to the inner wall and the other leaning against the outer wall (refer to Fig. 3 below). For Ha=20, the shape of the distribution of the contours changes completely, becoming elliptical near the inner wall and circular near the hot wall. As the Hartmann number increases, the maximum temperature is more distributed towards the outer wall.

Fig. 4 compares hybrid nanofluid with the base fluid via the local Nusselt number plotted at the inner wall (θ=0) when Ha=0. The close positioning of local Nusselt lines is observed, suggesting that the enhancement in heat transfer may not be deemed significant. However, it is noteworthy that marginal improvements in thermal transfer are demonstrated by the hybrid nanofluid compared to the base fluid.

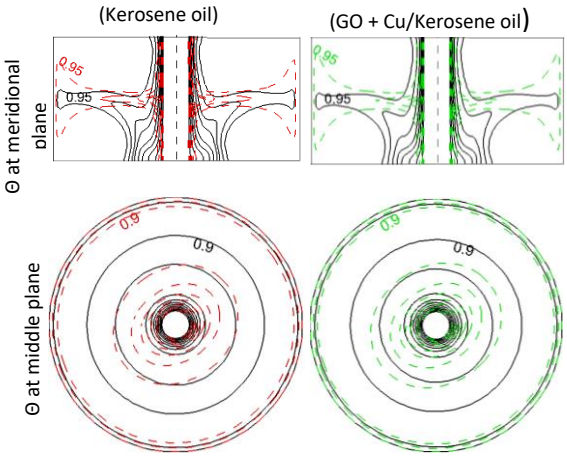

.

Fig. 3. Isotherms at meridional plane (top) and isotherms at middle plane (below) for (Kerosine oil), and hybrid nanofluid when Ha=0 and Ha=20

For a deeper understanding of this phenomenon, Fig. 5 depicts the spatial temperature structure at Θ = 0.95. A comparison between Kerosene oil and hybrid nanofluid when Ha=0 reveals that the highest temperature emerges in the central region, resembling a spinning top iso-surface. With increasing Hartmann number (Ha=20), subtle changes are observed for Kerosene oil, while the shape undergoes a complete transformation for the hybrid nanofluid. This transformation may be attributed to the weakening of buoyant forces, countered by the intensified Lorentz force, particularly pronounced due to the development of Hartmann layers near the inner and outer walls.

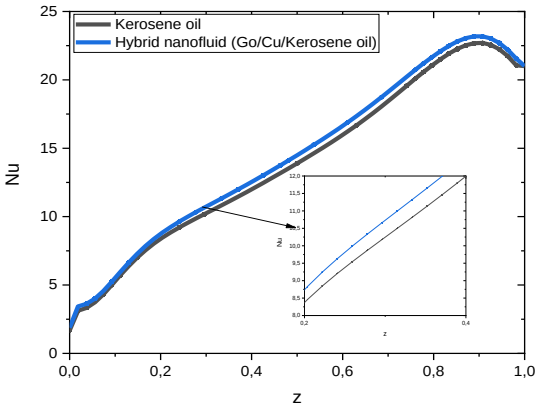

Fig. 4. Local Nusselt at Ha=0

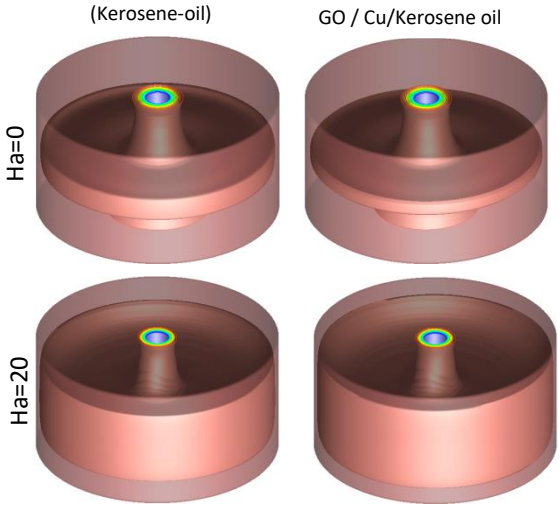

Fig. 5. Spatial structure of temperature for the iso-value Θ = 0.95.

To grasp the influence of an increased magnetic field on a hybrid nanofluid (GO/Cu/Kerosene oil), Fig. 6 presents a comparative analysis. The temperature and azimuthal velocity profiles at z = 1/2 are depicted for Hartmann numbers (Ha) of 20 and 40. Upon examining the structural cuts (r, θ), it becomes apparent that there exists a subtle discrepancy between Θ and w at Ha=20 and Ha=40. Notably, a significant disparity arises, particularly within the circular half-annulus,

where the temperature reaches its maximum value (Θ=0.95).

Conversely, the azimuthal velocity distribution displays a noticeable decline from the inner wall towards the midpoint of the annulus. This behavior can be explained by examining the areas near the rotating wall and those neighboring the inner wall, where electric current lines intersect perpendicularly with the magnetic field (B), resulting in an intensified Lorentz force. In summary, the observed fluctuations in temperature and azimuthal velocity under stronger magnetic fields can be attributed to the shifting dominance of electromagnetic forces over viscous forces with increasing Hartmann numbers, leading to distinct fluid behavior within the designated regions of the annulus.

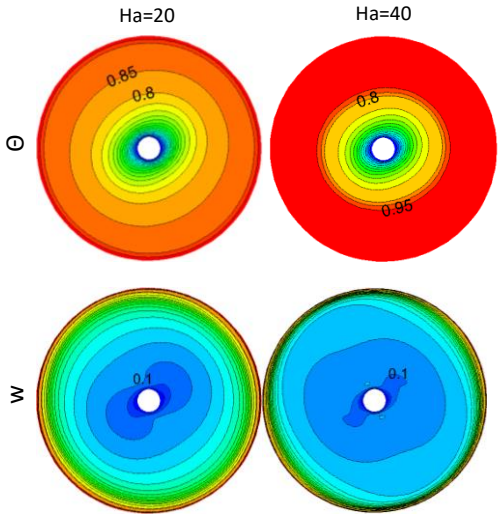

Fig.6. Comparison between Ha=0 and Ha=20 for hybrid nanofluid at the middle plane (z=1/2).

For more details, Fig.7 illustrates the influence of increasing the magnetic field intensity from 10 to 40. The profile of dimensionless azimuthal velocity w at r=0.2 (Fig.7a), and temperature plotted r=0.2 (Fig.7b) shows that increasing Ha has a double effect, one increases the velocity and decreases the temperature. The rise in azimuthal velocity (w) is more significant in the hybrid nanofluid. Conversely, the temperature reduction is more pronounced in the hybrid nanofluid than in the kerosene oil.

Fig. 7c showcases the influence of the Hartmann number (Ha) on the local Nusselt number at the inner wall (θ=0), comparing a hybrid nanofluid and a Copper nanofluid. The analysis indicates that the Nusselt number escalates with increasing Ha for both nanofluids. Particularly noteworthy is the more pronounced enhancement in the hybrid nanofluid when Ha=10, while nearly identical values are observed for both nanofluids when Ha=40. An intriguing observation is that the Nusselt profile attains its peak at the same heights (z=0.2 and z=0.8) and in z=1/2 it reaches a minimum.

4.3 Electrically conducting all walls

To gain a deeper insight into how electrical conductivity in the presence of a magnetic field influences convection in hybrid nanofluids, we assume perfect electrical conductivity for the inner and outer walls of the pool, excluding the bottom and top disks. In this scenario, according to the thin wall theory, the electric potential remains constant across the wall, indicating that the wall current density is tangential. It's important to highlight that the introduction of electrical conductivity to the inner and outer walls eliminates the presence of the Hartmann layer, allowing the fluid to move under the influence of inertial forces.

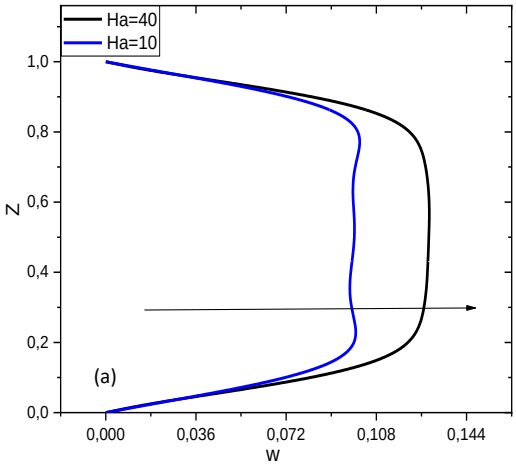

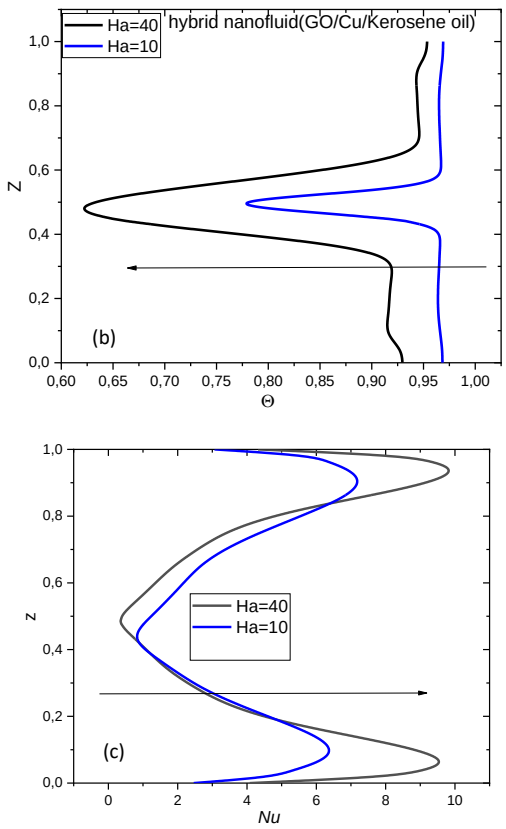

Fig. 7: (a) Dimensionless temperature, (b) Azimuthal velocity w at r=0.2, and (c) Local Nusset number at inner wall

To explore the impact of an increasing magnetic field on the flow field, Fig.8 compares the electric conductive walls case with earlier findings in the context of an insulating case. Isotherms contours are shown at the meridional plane (r=0) when Ha=10. The plot incorporates two cases: electrically insulating walls (EI), represented in the top, and electrically conducting walls (EC) represented below in Fig.8, superimposed on temperature (Θ) and azimuthal velocity (w) graphs. The temperature contours have a symmetrical shape in each case. For the (EC) case, the figure shows that the value Θ=0.95 in the case (EC) changes the position compared to the case (EI) and the large value of Θ takes a larger area for (EC). For the azimuthal velocity, the buoyant forces generated due to the fluid temperature differences cause the fluid to rise in the middle for the (EC) case.

Fig.9 compares two cases: electrically insulating walls (EI) and electrically conducting walls (EC) for two values Ha=10 and Ha=20. The profile of azimuthal velocity w (Fig.9a) and dimensionless temperature (Fig.9b) plotted at r=0.2 shows that increasing Ha has a double effect, one increases the velocity and decreases the temperature. Observations indicate that, in the scenario with (EC) and Ha=20, the temperature profile exhibits two peaks, with θ=0.42 at z=0.1 and Z=0.9. In contrast, in the case of (EI), a single peak with θ=0.2 is observed at z=0.5. For the profile of dimensionless azimuthal velocity in the case of (EC), the profile exhibits two peaks, for Ha=10 and Ha=40, respectively. The profile of w forms an arc with small values in comparison with the case (EC).

Fig. 9c shows magnetic damping in an electric conducting case (EC) and insulating one on the local Nusselt number at the inner wall (θ=0) when using a hybrid nanofluid. The observation reveals that the Nusselt number increases with the rising Ha from Ha=10 to Ha=40. Notably, there is a more significant enhancement in the hybrid nanofluid when the walls are electric conducting. The Nusselt profile reaches its maximum at the same heights (z=0.1 and z=0.9) and minimum at the midpoint of the annular pool (Z=1/2).

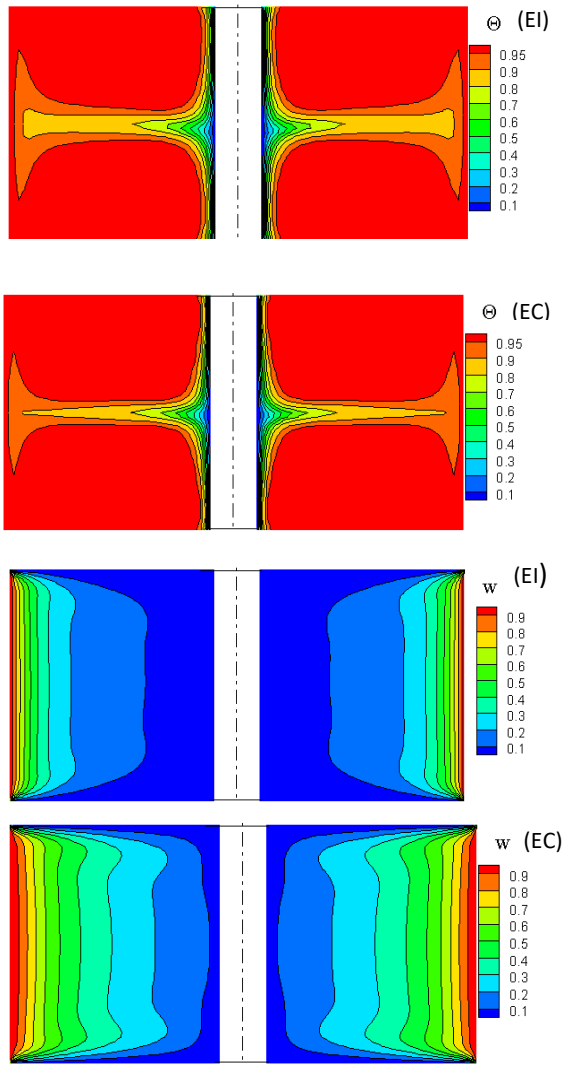

Fig.8. Isotherms (top) and azimuthal velocity (below) in plan (θ=0) for hybrid nanofluid in Ha=10, electrically insulating walls (EI)(top) and electrically conducting walls (EC) (below).

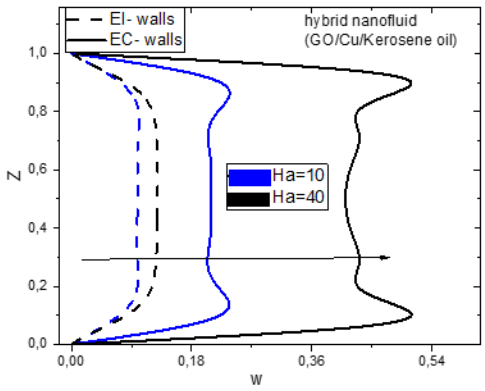

(a)

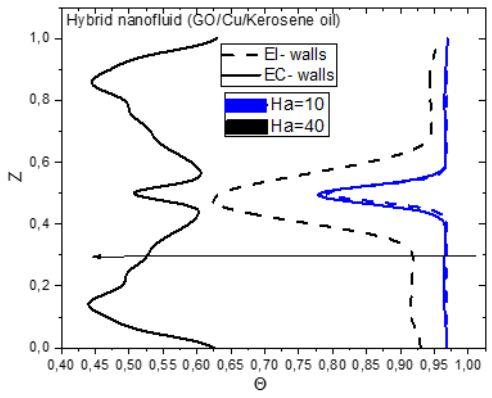

(b)

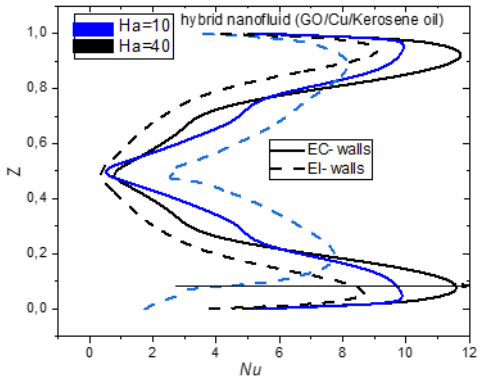

(c)

Fig. 9: (a) Dimensionless temperature, (b)Azimuthal velocity w at r=0.2, and (c) Nusselt number at inner wall (θ=0.)

Fig 10 presents the average Nusselt number versus Hartmann number (Ha) for kerosene oil and hybrid nanofluid (GO/Cu/kerosene oil). The average Nusselt number for the hybrid nanofluid is examined under two scenarios: electrically conductive (EC) and electrically insulating (EI) walls. It is observed that the Nusselt number monotonically increases with rising Ha and approaches a limiting value. Across all cases, the Nusselt number tends to peak between 6.5 and 7.5. Moreover, a prevalent trend of higher average Nusselt values is notable in the case of the hybrid nanofluid (GO/Cu/kerosene) compared to the base fluid, particularly evident when the walls are electrically conductive.

Fig.10 represents the evaluation of the average Nusselt as a function of Ha. With electrically conductive walls, the impact of the buoyancy force intensifies as the Hartmann

number increases, resulting in an increasingly significant interaction between the viscosity and buoyancy forces with increasing Ha. Therefore, it is inferred that the control of heat transfer performance is increasingly influenced by the combined effects of the magnetic field intensity and the electrical conductivity of the interior and exterior walls.

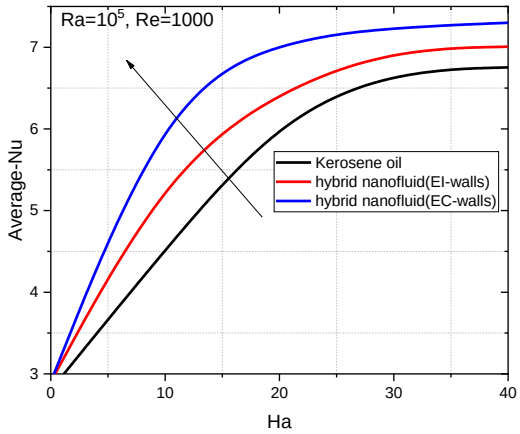

Fig. 10 Average Nusselt number versus Hartmann number at inner wall.

5. Conclusion

The numerical investigation delves into the swirling flow dynamics of hybrid nanofluid within the annular space between two coaxial cylinders, induced by the rotation of the outer wall. The system experiences bidirectional temperature gradients and a radial magnetic field. Employing the finite-volume method, the study solves the transport equations numerically. The analysis is given for kerosene oil, and hybrid nanofluid (GO/Cu/kerosene oil), focusing on isotherms, velocity profiles, local Nusselt, and average Nusselt numbers. The key insights from the investigation are summarized as follows:

- Without a magnetic field, the unchanged temperature distribution and heat transfer enhancements for the hybrid nanofluid do not exceed 20%.
- The introduction of a magnetic field symmetrically enhances the surface temperature distribution of hybrid nanofluid flow.
- Employing the hybrid nanofluid with higher magnetic field intensities raises the azimuthal velocities in the middle of the container.
- Optimal heat transfer is achieved with 90% improvement using the hybrid nanofluid when the walls of the annular space are electrically conductive.
- Recommendations for future research could include exploring alterations in the orientation of the magnetic field applied to coaxial cylindrical geometries containing a rotating hybrid nanofluid flow.

6. Acknowledgment

The authors gratefully acknowledge the support of the General Directorate of Scientific Research and Technological Development (Algeria).

References

[1] B. Mahfoud, Enhancement Heat Transfer of Swirling Nanofluid Using an Electrical Conducting Lid, Journal of Thermophysics and Heat Transfer 37(1) (2023) 263–271.

[2] H. Shao, W. Ma, M. Kohno, Y. Takata, G. Xin, S. Fujikawa, S. Fujino, S. Bishop, X. Li, Hydrogen storage and thermal conductivity properties of mg-based materials with different structures, Int. J. Hydrog. Energy 39 (2014) 9893–9898

[3] H. Arasteh, R. Mashayekhi, D. Toghraie, A. Karimipour, M. Bahiraei, A. Rahbari, Optimal arrangements of a heat sink partially filled with multilayered porous media employing hybrid nanofluid, J. Therm. Anal. Calorim. 137 (2019) 1045–1058,

[4] M.H. Esfe, H. Hajmohammad, D. Toghraie, H. Rostamian, O. Mahian, S. Wongwises, Multi-objective optimization of nanofluid flow in double tube heat exchangers for applications in energy systems, Energy 137 (2017) 160–171.

[5] L. Bouragbi, A. Salaheddine, B. Mahfoud, Analyses of entropy generation for a solar minichannel flat plate collector system using different types of nanofluids, Journal of Computational Applied Mechanics 52(4) (2021), 664-681,

[6] S. Ghadikolaei, K. Hosseinzadeh, D.D. Ganji, Investigation on ethylene glycolwater mixture fluid suspend by hybrid nanoparticles (TiO2-CuO) over rotating cone with considering nanoparticles shape factor,Journal of Molecular Liquids, 272 (2018) 226–236

[7] M.H. Esfe, S. Esfandeh, M.K. Amiri, M. Afrand, A novel applicable experimental study on the thermal behavior of SWCNTs (60%)-MgO (40%)/EG hybrid nanofluid by focusing on the thermal conductivity, Powder Technology, 342, (2019) 998–1007

[8] A. Moradi D., Toghraie, A.H.M. Isfahani, A. Hosseinian, An experimental study on MWCNT–water nanofluids flow and heat transfer in double-pipe heat exchanger using porous media, Journal of Thermal Analysis and Calorimetry, 137, (2019) 1797–1807

[9] Z. Mahmood, Z. Iqbal, M. Ahmed Alyami, B. Alqahtani, M. Yassen, U. Khan, Influence of suction and heat source on MHD stagnation point flow of ternary hybrid nanofluid over convectively heated stretching/shrinking cylinder, Advances in Mechanical Engineering, 14 (2022) 1–17

[10] M.Khan, M.N. Tahir, S.F. Adil, H.U. Khan, M.R. Siddiqui, M. Kuniyil, W.Tremel, Graphene based metal and metal oxide nanocomposites: Synthesis, properties and their applications, Journal of Materials Chemistry A, 3, (2015) 18753–18808.

[11] S.S. Ghadikolaeia, M. Gholiniab, 3D mixed convection MHD flow of GO- MoS2 hybrid nanoparticles in H2O– (CH2OH)2 hybrid base fluid under effect of H2 bond, International Communications in Heat and Mass Transfer, 110, (2020) 104371.

[12] B. Ruhani D. Toghraie M. Hekmatifar M. Hadian, Statistical investigation for developing a new model for rheological behavior of ZnO–Ag (50%–50%)/Water hybrid Newtonian nanofluid using experimental data, Physica A: Statistical Mechanics and its Applications, Vol. 525, (2019) 741–751.

[13] B. Mahfoud, Magnetohydrodynamic effect on vortex breakdown zones in coaxial cylinders, European Journal of Mechanics-B/Fluids (89) (2021) 445–457

[14] H. Benhacine, B. Mahfoud, M. Salmi ,Stability effect of an axial magnetic field on fluid flow bifurcation between coaxial cylinders, International Journal of Computational Materials Science and Engineering 10(4) (2021) 2150023

[15] B. Mahfoud., H. Benhacine, A. Laouari, A. Bendjaghlouli, Magnetohydrodynamic Effect on Flow Structures Between Coaxial Cylinders Heated from Below, Journal of Thermophysics and Heat Transfer 34(2) (2019) 1-10.

[16] B. Mahfoud, A. Laouari, A. Hadjadj, H. Benhacine, Counter-rotating flow in coaxial cylinders under an axial magnetic field, European Journal of Mechanics-B/Fluids (78) (2019) 139-146.

[17] M. Azzoug, B.Mahfoud, Hibet. E. Mahfoud, Influence of External Magnetic Field on 3D Thermocapillary Convective Flow in Various Thin Annular Pools Filled with Silicon Melt, Journal of Applied Fluid Mechanics, Vol. 16 (2023) pp. 1853-1864

[18] M. Moussaoui, B. Mahfoud, Hibet E. Mahfoud, Using a Magnetic Field to Reduce Thermocapillary Convection in Thin Annular Pools, Journal of Thermophysics and Heat Transfer,37 (4) (2023)

[19] B. Mahfoud, O.M. Azzoug, MHD effect on the thermocapillary silicon melt flow in various annular enclosures, Crystal Research & Technology, 58 (6) (2023)

[20] A. Bendjaghlouli, D.E. Ameziani, B. Mahfoud, L. Bouragbi, Magnetohydrodynamic Counter Rotating Flow and Heat Transfer in a Truncated Conical Container, Journal of Thermophysics and Heat Transfer 33(3) (2019) 365-374.

[21] H. Benhacine, B, Mahfoud, M. Salmi, Stability of conducting fluid flow between coaxial cylinders under thermal gradient and axial magnetic Field, International Journal of Thermofluid Science and Technology 9(2) (2022) 090202.

[22] B. Mahfoud, Magnetic Field Effect on Natural Convection in Trapezoidal Geometry**,** https://www.researchgate.net/publication/369040424, (2023).

[23] B. Mahfoud, Simulation of Magnetic Field Effect on Heat Transfer Enhancement of Swirling Nanofluid" International Journal of Computational Materials Science and Engineering, 11 (4) (2022) 2250007.

[24] B. Mahfoud, A. Bendjaghloli, Natural convection of a nanofluid in a conical container, Journal of Thermal Engineering, 4, (2018) 1713-1723.

[25] B. Mahfoud, Effect of Wall Electrical Conductivity on Heat Transfer Enhancement of Swirling Nanofluid-Flow, Journal of Nanofluids, 12, (2023) 418-428.

[26] M. Mollamahdi, M. Abbaszadeh, G. A. Sheikhzadeh, Flow field and heat transfer in a channel with a permeable wall filled with Al2O3-Cu/water micropolar hybrid nanofluid, effects of chemical reaction and magnetic field, Journal of Heat and Mass Transfer Research, 3 (2016) 101- 114.

[27] M.A. Mansour, S. Sadia, R. Gorla, A.M. Rashad, Effects of heat source and sink on entropy generation and MHD natural convection of Al2O3-Cu/water hybrid nanofluid filled with square porous cavity, Thermal Science and Engineering Progress, 6, (2017) 57-71.

[28] A. Alsaedi, K. Muhammad, T. Hayat, Numerical study of MHD hybrid nanofluid flow between two coaxial cylinders, Alexandria Engineering Journal, 61 (2022) 8355–8362,

[29] Y. Shagaiya Daniel., Z. Abdul Aziz, Z.Ismail, A. Bahar, F.Salah, Slip role for unsteady MHD mixed convection of nanofluid over stretching sheet with thermal radiation and electric field, Indian Journal of Physics. (2019) May:1-3.

[30] Y. Shagaiya Daniel., Z. Abdul Aziz, Z.Ismail, A. Bahar, F.Salah, Stratified electromagnetohydrodynamic flow of nanofluid supporting convective role, Korean Journal of Chemical Engineering. (2019) 1;36(7):1021-32.

[31] Y. Shagaiya Daniel., S.K. Daniel, Effects of buoyancy and thermal radiation on MHD flow over a stretching porous sheet using homotopy analysis method. Alexandria Engineering Journal.(2015) 1;54(3):705-12.

[32] Y. Shagaiya Daniel., Z. Abdul Aziz, Z.Ismail, A. Bahar, F.Salah, Entropy analysis in electrical magnetohydrodynamic (MHD) flow of nanofluid with effects of thermal radiation, viscous dissipation, and chemical reaction. Theoretical and Applied Mechanics Letters.(2017) 1;7(4):235-42.

[33] Y. Shagaiya Daniel, Z. Abdul Aziz, Z.Ismail, A. Bahar, F. Salah, Effects of slip and convective conditions on MHD flow of nanofluid over a porous nonlinear stretching/shrinking sheet. Australian Journal of Mechanical Engineering. (2018) 2;16(3):213-29.

[34] S. Manjunatha, B. Ammani Kuttan , S. Jayanthi , Ali Chamkha, B.J. Gireesha e Heat transfer enhancement in the boundary layer flow of hybrid nanofluids due to variable viscosity and natural convection. Heliyon 5 (2019) e01469.

[35] G. Kotha, V.R. Kolipaula, S. Rao Venkata, M. Surekha Penki and Ali J. Chamkha. Internal heat generation on bioconvection of an MHD nanofluid flow due to gyrotactic microorganisms, The European Physical Journal Plus (2020) 135(600)

[36] M. Veera Krishna & Ali J. Chamkha, Hall and ion slip effects on Unsteady MHD Convective Rotating flow of Nanofluids—Application in Biomedical, Engineering . Journal of the Egyptian Mathematical Society, 28 (2020) number: 1

[37] F. Madani, B. Mahfoud, Hibet E. Mahfoud, Influences of electrical conductivity of the cylindrical walls on heat transfer enhancement of nanofluid swirling flow" International Journal of Thermofluid Science and Technology, 10, (2023) 100201

[38] H. Benhacine., B. Mahfoud., M. Salmi, Stability of an Electrically Conducting Fluid Flow between Coaxial Cylinders under Magnetic field, Journal of Applied Fluid Mechanics, 15 (2022) 1741-1753